ELSEVIER Applied Catalysis B: Environmental 12 (1997) 161–191

APPLIED CATALYSIS B: ENVIRONMENTAL

Development and application range of mathematical models for 3-way catalytic converters

G.C. Koltsakis, P.A. Konstantinidis, A.M. Stamatelos *

Laboratory of Applied Thermodynamics, Aristotle University Thessaloniki, 540 06 Thessaloniki, Greece

Received 18 March 1996; revised 7 July 1996; accepted 23 July 1996

Abstract

The need for reliable 3-way catalytic converter modeling in the design of demanding exhaust systems for low-emitting vehicles has been widely recognised. Although a number of related models have been presented in the literature, the efficient performance in actual 3-way applications requires further development and validation. The major difficulties posed in such modeling efforts arise from the complexities in the reaction schemes and the respective rate expressions for the multitude of currently used catalytic formulations. This paper presents a two-dimensional catalytic converter model, featuring a number of innovations regarding the catalyst transient behaviour, the reaction kinetics and the solution procedure. The oxygen storage submodel presented is capable of accounting for the redox and temperature dependence of the oxygen availability under transient operation. The redox sensitivity of the reaction scheme gives a clearer insight in the 'lambda-window' behavior of 3-way catalysts. The application range of the model and the expected accuracy levels in the most common engineering problems are discussed. It is concluded, that although the task of predicting emissions over random driving scenarios is quite demanding in both chemical kinetics and inlet conditions data, most optimization applications may be sufficiently handled with existing kinetic expression information.

Keywords: Automotive emissions; Converters; Mathematical modeling; Reaction kinetics; Design optimization

1. Introduction

Mathematical modeling of monolithic catalytic converters is employed during more than 20 years to assist the design and development of automotive exhaust

* Corresponding author. Tel.: (+30-31) 996066; fax: (+30-31) 996019; e-mail: tassos@antiopi.meng.auth.gr.

PII S0926-3373(96)00073-2

after-treatment systems. In a pioneering work, Young and Finlayson [1] have developed and solved a two-dimensional channel model for a monolith using orthogonal collocation. They discussed in detail the applicability of the quasi-static assumption for the gas phase for transient cases. Heck et al. [2] showed that a simpler one-dimensional model is adequate for predicting monolith behavior. Lee and Aris [3] reported a two-dimensional, two phase model that also included heat radiation effects. Otto and LeGray [4] validated their model with experimental results and presented model predictions regarding the converter efficiency for different exhaust system designs. Their model included also radial conduction effects in the monolith.

Oh et al. presented a model for the pellet type catalyst in [5]. Extensive verification of this model by engine bench experiments is given in [6]. This model was employed for the prediction and parametric analysis of vehicle exhaust emissions during the warm-up [7]. The same authors studied the response of a monolithic catalytic converter to step changes in feedstream temperature using a one-dimensional adiabatic channel model [8].

Most of the above mentioned modeling studies were focused on the behavior of adiabatic monoliths exposed to a uniform flow distribution at the front face. In this case, temperature and concentration profiles in all channels of the monolith are the same, so that consideration of only one channel would be sufficient. However, actual automobile converters operate in a non-adiabatic mode under conditions where the gas flow is distributed non-uniformly at the monolith inlet. Flytzani-Stephanopoulos et al. [9] dealt with the two-dimensional (axi-symmetric) heat transfer process in a non-reactive monolith. Becker and Zygourakis [10] presented two-dimensional solutions for an adiabatic reacting monolith using a simplistic reaction scheme considering only CO oxidation and neglecting the effects of heat transfer through the surrounding materials. Chen et al. [11] developed a comprehensive three-dimensional model for the analysis of transient thermal and conversion characteristics of monolithic catalytic converters.

The models mentioned above relied on the historical data provided by Voltz et al. in [12] which refer to CO and HC oxidation in a lean environment on a platinum catalyst. The rate expressions are of the Langmuir–Hinshelwood type and account for the inhibition due to NO. Although this approach was sufficient for modeling oxidizing catalytic converters, 3-way catalytic converter modeling should account for the reaction mechanisms in operating conditions very close to stoichiometry, which pose additional challenges, as will be discussed below.

Chen and Cole [13] validated their model by measurements on a Pt/Rh monolithic converter and modified the kinetic expressions to achieve better agreement with the results of full-scale experiments on an engine. In a paper assessing potential exhaust after-treatment technologies, Gottberg et al. [14] mentioned a more detailed channel model, which took into account independently adsorption from gas phase to surface site, surface reactions ('electron

transfer') and desorption from surface to gas phase for the following 5 chemical species: CO, CO_2, O_2, NO and C_3H_8. Naturally, the authors could not find kinetics data to sufficiently cover such a complex model. They conducted extensive trial simulation work aiming at the achievement of a satisfactory model validation against real emission data under different dynamic conditions, using minor (empirical) adjustments of adsorption, desorption and reaction rate constants. Montreuil et al. [15] presented a concerted effort aiming at the compilation of an experimental database of steady-state catalyst conversion efficiency for two catalyst formulations, for the purpose of updating the kinetic rate constants in the Ford 3-WCC model [4]. They employed the so far most inclusive reaction scheme comprising 13 reactions and derived redox dependent kinetic expressions, which are valid above 371°C.

Pattas et al. [16] presented a transient 1-D modeling approach for the 3-WCC embodying an oxygen storage and release submodel. The model relied on a simplified 5 reaction scheme comprising CO, H_2 and HC oxidation and NO reduction by CO. A similar approach for the reaction scheme, lacking oxygen storage, was presented in [17]. This category of models are routinely used by auto-manufacturers for design optimization of exhaust after-treatment systems based on 3-WCCs.

The main problem in the evolution of this category of transient 3-WCC models is the lack of adequate kinetics data covering a significant number of reactions, for the multitude of catalyst formulations and washcoats employed in automotive applications. Moreover, the situation is further complicated by the effect of various modes and degrees of catalyst ageing during vehicle operation. For this reason, it has become common practice to rely on tunable kinetics expressions, which should supply a satisfactory number of degrees of freedom for the model [18]

The validity of this approach in supporting assessment and design optimization has been illustrated for some cases involving conventional single converter exhaust systems. The stricter emission standards already put into effect require more careful design, often including major modifications, such as pre-converters or electrical heating for the minimization of the catalyst cold operating phase. In these cases the accuracy requirements of mathematical models are definitely increased. To this end, this paper presents a comprehensive 2-dimensional mathematical model of the catalytic converter featuring an extended reaction scheme and an improved oxygen storage submodel for highly transient catalyst operation. The model presentation is preceded by a brief discussion on the physical and chemical phenomena taking place in the catalytic converter and a short review of the existing modeling approaches. A number of practical modeling applications are presented and discussed in terms of expected prediction accuracy, input data requirements and model limitations, aiming at the investigation of the scope and extends of model application in automotive catalysis.

2. Phenomena involved in 3-WCC operation

In this section, the main physical and chemical phenomena affecting 3-WCC operation will be recognized and discussed in order to assess their importance in related mathematical models. The analysis includes a brief review of the main modeling approaches used for each phenomenon.

2.1. Heat and mass transfer

Although the flow in the exhaust piping of an engine is normally turbulent, the Re numbers in the converter monolith channels are always safely in the laminar region ($20 < \mathrm{Re} < 300$). The gas velocity at the channel entrance is assumed to have a plug flow profile, which develops hydrodynamically to the parabolic profile over the entrance length. In this region, which extends to a few millimeters after the monolith entrance, the transport phenomena are enhanced.

Two general directions in the modeling of the transport processes in the monolithic channels have appeared in the related literature. Simultaneous 3-D solution of the energy and mass balance equations of the boundary layer assuming a parabolic velocity profile has been presented in [1]. The simplified approach of employing the well-known Nu and Sh functions for the flow in closed ducts has been followed in the great majority of the 3-WCC models presented. The latter approach offers simplified, less time-demanding 1-D handling and practically equivalent accuracy levels.

In many of the 1-D mathematical models presented so far, the Nu and Sh numbers have been considered constant along the channel, and their value equals that corresponding to the solution of the Graetz–Nusselt problem for constant wall temperature. In order to take account for the transfer rates augmentation found in the entrance region, spatial dependent values of Nu and Sh can be used. For example, Hawthorn proposed the following relation for Nu number for laminar flow in ducts [19]

$$\mathrm{Nu} = 2.976\left(1 + \frac{0.095}{x^*}\right)^{0.45} \tag{1}$$

Analogous relations can be used for the mass transfer, employing the heat-mass transfer analogy [20]. It should be noted, that the heat and mass transfer analogy is only technically correct when the boundary conditions for the heat and mass transfer problems are the same. This is, however, not always the case with 3-way catalytic converter applications.

Two dimensional solutions of the heat and mass boundary layers have been employed to study the variation of Nu and Sh numbers along the channel [2], [21], [22], [23]. Groppi et al. [23] suggested that the Nu number approximates the solution of the Graetz–Nusselt problem for constant heat flux when the reaction

is kinetically controlled, whereas in the mass diffusion control region the solution for constant wall temperature is more realistic. Hayes and Kolackowski [22] have reported some unusual behavior of the Nu and Sh numbers during transient operation in the region where the reaction becomes mass-diffusion limited. Furthermore, the actually non-uniform washcoat deposition on the channel walls results in geometries, which are not exactly square. These effects cannot be predicted using 1-D channel models. However, it has been shown that for typical applications in square channels, minor differences (10–15 K) in the predictions of 1-D (lumped) vs. 2-D (distributed) models are observed in terms of gas temperatures for a variety of parameter values [23]. The above investigations justify the use of asymptotic solutions for the Nu and Sh numbers by 1-D channel models, which are also employed in the present model.

Apart from the convective heat exchange between the exhaust gas and the substrate, heat is additionally generated from the exothermic reactions of some exhaust pieces (CO, hydrocarbons) on the catalytic washcoat. In the case of electrically heated catalysts, electrical energy is supplied to the substrate in order to quicken its temperature rise during warm-ups. At high operation temperatures, heat radiation from the substrate to the surrounding walls should also be mentioned. Heat radiation inside the substrate channels can be important, when large temperature gradients along the channel are present [3]. The converter heat losses to ambient occur via convection (free and forced) and radiation from the converter shell.

The concentration gradients between the flowing gas and the reactive washcoat induce the convective mass transfer in the monolith channels. Since the species of interest are present in low concentrations in the exhaust gas of a gasoline engine, the mass transfer is governed by the laws of diffusion in dilute mixtures [20]. The diffusion in the reactive washcoat is likely to limit the overall reaction rates at temperatures higher than 700 K [22]. These effects are also complicated by the non-uniform washcoat deposition in the channel walls, since the major quantity of the washcoat is deposited near the channel corners. In the majority of the models the washcoat layer is considered thin and the effectiveness factor equal to 1. This approach is followed in the present model.

2.2. *Inlet flow distribution*

Non-uniformities in the velocity field at the inlet of the converter may cause both poor converter performance due to localized high space velocities and increased ageing due to poison accumulation in high mass flow rate areas of the monolith [24]. Consequently, a large amount of computation and experimental work has been conducted so far, aiming at the minimization of the flow maldistribution [25,26]. An outcome of these studies is related to the quantification of maldistribution by means of semi-empirical indices, which correlate well with the flow Re numbers and monolith and diffuser geometry. The effects of

flow maldistribution on the overall catalyst efficiency and ageing should be taken into account in any modeling methodology.

2.3. Chemical kinetics

The multitude of the heterogeneous reactions taking place on the catalytic washcoat poses a challenge for the engineer involved in the design, modeling and manufacturing of 3-way catalytic converters. Converter models require reliable kinetic expressions that account for the composition and temperature dependence of the reaction rates. The kinetic expressions should be conveniently formed in order to allow model flexibility in matching behaviour of a large variety of catalyst formulations and washcoats.

In [12] extensive measurements on pellet-type Pt catalysts are processed to derive kinetic rate expressions for the oxidation reactions of CO and C_3H_6 under oxygen rich conditions. These relations are of the Langmuir–Hinshelwood type and account for the inhibition of CO, C_3H_6 and NO. According to this theory, the inhibition is essentially governed by the adsorption characteristics at equilibrium without reaction. Consequently, measurements of adsorption isotherms under non-reacting conditions yield in principle the adsorption constants involved in an L–H expression. A numerical integration–optimization computer program was used to find the best combination of kinetic parameters for a given set of rate equations of this type.

Due to the absence of analogous works for other types of catalysts, the above mentioned rate expressions — with minor modifications — have been extensively used by almost all models developed since then. Proceeding further towards the case of a three-way catalyst, the first rate expressions concerning the simultaneous oxidation of CO and reduction of NO were provided in [27]. Here again, the expressions are of the Langmuir–Hinshelwood type, but they also involve fractional and positive orders which are of empirical nature. Montreuil et al. in [15] presented a method to tune a mathematical model in order to best represent the steady-state conversion characteristics of Pt/Rh and Pd/Rh catalysts under a variety of redox and temperature conditions. This method involved 13 reactions and 97 independent tunable parameters for the kinetic rate expressions.

As mentioned above, most of recent mathematical models rely on the Langmuir–Hinshelwood type expressions given in [12] for the CO and hydrocarbon oxidation with modified activation energies and activity factors, best suited to the activity of the catalyst modeled. It appears, that this approach is acceptable since it provides the required accuracy levels, at least under the operating conditions met in the most common automobile applications [16].

The reaction mechanisms involved in NO reduction are more complicated. Oh studied the reaction CO–NO on a Rh catalyst and derived activation energies and reaction orders for a variety of washcoat supports under CO excess

(rich) conditions [28]. In order to extend this kinetics data to the lean region, one may refer to [29], where a series of measured rate data regarding CO–NO reaction is presented in binary mixtures and in the presence of O_2 on a Pt/Rh catalyst. At relatively high temperatures (above 400°C) an apparent first-order kinetic for CO is found until complete consumption of one reaction partner near the surface enforces approximately zero-order kinetic. In fact, due to additional inhibition of the reaction, a slightly negative order is identified, which is in agreement with the findings presented in [28].

2.4. Oxygen storage

In most current technology gasoline cars the signal of the lambda sensor [30] is used as a feedback control signal for the fuel injection system in order to ensure that a stoichiometric fuel–air mixture is supplied in the cylinders. However, the system's response lag (mainly attributed to the exhaust gas travel time and the sensor's response delay) causes the air-to-fuel ratio to oscillate around the stoichiometric value with the limit cycle frequency of the control system.

The behavior of the 3-way catalytic converter under such dynamic conditions presents therefore high practical interest. Since the beginning of the previous decade, it has been recognized that the 3-way catalyst efficiency is significantly affected when the composition of the feed gas is modulated with different amplitudes and frequencies [31–35]. This behavior is mainly attributed to the ability of some washcoat components to be periodically oxidized and reduced depending on the exhaust gas redox environment. For example, the activity of the noble metals Pt, Pd and Rh depends on their oxidation state and is lowered for higher oxidation levels [36], [37].

The washcoat component, that seems to play the most important role in these dynamic oxidation–reduction phenomena is cerium. Cerium is normally present in high quantities in the washcoat (order of 30 wt.-% or 1000 g/ft^3) and has multiple functions: stabilization of the washcoat layer and improvement of thermal resistance [36], enhancement of precious metal catalytic activity [28] and function as an oxygen storage component.

The experimental studies of Herz in [38] showed that oxygen adsorption and desorption phenomena under periodically varying inlet conditions are attributed to the presence of cerium and to a much lesser extend to other washcoat species. The function of cerium as oxygen storage component is based on its ability to form both 3- and 4-valent oxides. Under net oxidizing conditions the following Ce oxide reactions may take place:

$$Ce_2O_3 + 1/2O_2 \rightarrow 2CeO_2 \quad (2)$$

$$Ce_2O_3 + NO \rightarrow 2CeO_2 + 1/2N_2 \quad (3)$$

$$Ce_2O_3 + H_2O \rightarrow 2CeO_2 + H_2 \quad (4)$$

On the other hand the CeO_2 may function as an oxidizing agent of the exhaust gas species under net reducing conditions according to the following reactions:

$$2CeO_2 + CO \rightarrow Ce_2O_3 + CO_2 \quad (5)$$

$$2CeO_2 + H_2 \rightarrow Ce_2O_3 + H_2O \quad (6)$$

The oxygen storage availability is apparently a function of the washcoat Ce content and dispersion. Moreover, the stored oxygen available to react under operating conditions is a function of the local temperature and redox environment [39].

3. Model description

3.1. Model equations

A two-dimensional axi-symmetric grid is used to model the catalytic converter. Catalytic monoliths of non-cylindrical shape are simulated by cylindrical ones with equal frontal area and length. Thus the employment of a 3-dimensional grid that would considerably burden the computation effort is avoided. Previous studies on 2-D grids [11] and experience with 1-D models [16] indicate that this assumption does not seriously affect the desired accuracy levels. In the radial direction the grid is non-uniform being denser in the region of the external insulation. With a given temperature and velocity distribution at the monolith inlet, representative inlet conditions can be defined for all channels contained in each monolith zone. Each time marching comprises the solution of the balance equations describing the transport and chemical phenomena for one channel per zone and the temperature field computation in the converter. The basic features of the mathematical model are as follows:

(i) computation of the convective heat and mass transfer from the exhaust gas to the catalytic surface. A 'film approach' is adopted employing mean bulk values for the gas phase and solid–gas interface values for the solid phase species concentrations. The corresponding transfer coefficients are computed using spatially dependent relations for Nusselt and Sherwood numbers applicable to laminar flows in ducts. Axial diffusion in the gas phase is ignored, due to the very low Pe numbers found in operating conditions;

(ii) computation of the heterogeneous chemical reactions taking place on the catalytic surface based on Langmuir–Hinshelwood based rate expressions. 'Lumping' of surface adsorption–desorption and pore diffusion phenomena in the kinetic rate expressions. The reaction scheme adopted is presented below. Neglecting of the contribution of homogeneous reactions since their reaction rates are important only at unusually high temperatures;

(iii) the 2-D transient temperature field in the cylindrical converter is computed taking into account the heat conduction in the substrate and the surrounding insulation and the heat losses to the surroundings via convection and radiation. The contributions of the convective heat transfer in the channels and the exothermic heat release are taken into account by the respective source terms;

(iv) the oxygen storage and release phenomena in the washcoat are described by the dynamic redox activity of the cerium oxides present in the catalytic layer. Tunable kinetic rate expressions are employed to represent catalyst performance in a wide range of temperature and redox environments.

The transient behavior of the catalytic converter is computed as a series of quasi steady-states. This approach is valid since the characteristic time constants involved in the transport and reaction phenomena are typically much smaller than the characteristic period of the unsteadiness of the inlet conditions found in automobile applications. It is assumed that during a single time marching, the temperature of the solid phase remains unchanged, which is realistic due to the typically slower response of the solid phase. An analogous treatment is used to compute the time variation of the oxidation fraction of the oxygen storage component, as will be discussed in detail below. Based on the above assumptions, the solution procedure followed in each time step may be divided in the following stages:

(i) computation of the temperature in the gas phase along a representative channel for each zone;

(ii) application of mass balances and reaction kinetic expressions to calculate the resulting composition changes along the channel in the gas and solid phases;

(iii) solution of the two-dimensional temperature field in the converter taking into account the appropriate source terms due to the convective heat transfer and the exothermic heat release.

The first stage involves the computation of the gas temperature for each node $i+1$ given the conditions in the node i. Employing locally analytical solutions based on the 'number of transfer units' (NTU), we obtain:

$$T_{g,i+1} = T_{s,i} + \left(T_{g,i} - T_{s,i}\right)\mathrm{e}^{-\mathrm{NTU}_h} \tag{7}$$

with the NTU number defined as:

$$\mathrm{NTU}_h = \frac{h \cdot \Delta F}{\dot{m} \cdot C_{p,g}} \tag{8}$$

After the determination of the temperature distribution along the channel, the corresponding heat fluxes may be computed for each space step according to the following balance equation:

$$\dot{q}_{\mathrm{conv},i} = \frac{\dot{m}_g \cdot C_{p,g}}{\Delta V_r}\left(T_{g,i} - T_{g,i+1}\right) \tag{9}$$

Combining (7) with (9) we can express the convective heat fluxes at node i using local variables:

$$\dot{q}_{\mathrm{conv},i} = \frac{\dot{m}_g C_{p,g}}{\Delta V_r}(T_{g,i} - T_{s,i})(1 - \mathrm{e}^{-\mathrm{NTU}_h}) \tag{10}$$

The employment of locally analytic solutions presents substantial stability advantages over the classical approaches used in previous models. The computation of the gas temperature during the space marching is not subject to virtually any constraints regarding the space step, since the form of Eq. (7) prohibits computation of thermodynamically invalid temperatures. Similar considerations apply also for the treatment of the mass balances presented below.

The mass balance equations for each exhaust gas species j employing again the NTU number yields:

$$c_{g,i+1} = c_{s,i} + (c_{g,i} - c_{s,i})\mathrm{e}^{-\mathrm{NTU}_m} \tag{11}$$

with

$$\mathrm{NTU}_m = \frac{k \cdot \rho_g \cdot \Delta F}{\dot{m}_g} \tag{12}$$

The local molar fluxes for each species per unit reactor volume are:

$$\dot{n}_i = \frac{\dot{m}_g}{\Delta V_r M_g} \cdot (c_{g,i} - c_{g,i+1}) \tag{13}$$

Combining Eq. (10) and Eq. (13) we express again the molar fluxes using local variables:

$$\dot{n}_i = \frac{\dot{m}_g}{\Delta V_r M_g}(c_{g,i} - c_{s,i})(1 - \mathrm{e}^{-\mathrm{NTU}_m}) \tag{14}$$

The above mass balance equations apply for all the chemical species considered, although the subscripts have been omitted for convenience.

Based on the quasi-steady assumption stated above, we can compute the concentrations at the solid–gas interface and the resulting reaction rates by equating the diffusion and the reaction rates for each species j under consideration:

$$\dot{n}_{i,j}(c_{g,i,j}, c_{s,i,j}) = R_{i,j}(\bar{c}_{s,i}, T_{s,i}) \tag{15}$$

According to Eq. (15), the rates of reaction and mass transfer to the catalytic surface are always in equilibrium, implying that there is no species accumulation on the solid catalytic surface. This assumption is realistic for steady-state operation, but not necessarily for operation under a highly transient temperature and composition conditions. In the latter case, the employment of Eq. (15) with Langmuir–Hinshelwood type expressions for the reaction rates would probably

not be sufficient. In order to account for the effects of transient adsorption–desorption and heterogeneous reaction phenomena, the kinetic model should include the detailed computation of the time-dependent surface coverage of each species on the active sites. Such models have been presented by a number of researchers [40,41] for the case of a 1-D isothermal reactor with simple gas mixtures (up to three reacting species). These models aim at studying the effects of oscillatory equivalence ratio on catalyst performance. However, the number of kinetic parameters needed for such a task are numerous and very difficult to estimate. In our model, the quasi-steady approach expressed by Eq. (15) is retained, while highly transient effects are taken into account by focusing on the well-known oxygen storage effects, which are probably the most dominant for practical application cases [42]. This aims at keeping model complexity, and thus flexibility, to acceptable levels, at the same time profiting from the available experience regarding L–H kinetic rate expressions for 3-way catalysts.

The reaction rates R_j are complex functions of the local temperature and composition at the gas–solid interface and are discussed in more detail in the following sub-section. For the species participating in more than one reaction, the rate is computed as the sum of the individual reaction rates.

From Eq. (14) and Eq. (15) using the parameter W defined in the nomenclature, we came to a system of non-linear equations of the form:

$$W_{i,j}(c_{g,i,j} - c_{s,i,j}) = R_{i,j}(\bar{c}_{s,i}, T_{s,i}) \tag{16}$$

With the solid temperatures $T_{s,i}$ and gas phase concentrations $c_{g,i,j}$ known, Eq. (16) represents a system of non-linear equations, which can be solved by the Newton's method at each node i to obtain the solid phase concentrations. Then, we can march to the next space step by computing the gas phase concentrations according to Eq. (11).

The temperature field in the converter is described by the equation of transient heat conduction with heat sources in cylindrical co-ordinates:

$$\rho_s C_{p,s} \frac{\partial T_s}{\partial t} = \lambda_{s,x} \frac{\partial^2 T_s}{\partial x^2} + \lambda_{s,r} \frac{1}{r} \frac{\partial}{\partial r}\left(r \frac{\partial T_s}{\partial r} \right) + S \tag{17}$$

The values of ρ_s, $C_{p,s}$, $\lambda_{s,x}$, $\lambda_{s,r}$ depend on the respective grid node. As explained above, apart from the monolithic substrate the grid contains the insulating layer and canning. The nodes included in the substrate bulk values are taken for the above parameters, according to the void fraction of the substrate. The source term S includes the contribution of the convective heat transfer of the flowing gas, the exothermic heat release as well as possible external electrical heating:

$$S = \dot{q}_{\text{conv}} + \dot{q}_{\text{el}} + \sum_{k=1}^{6} (-\Delta H_k) \cdot R_k \tag{18}$$

The boundary conditions for the heat conduction equation are:

$$\lambda_r \frac{\partial T}{\partial r} = h_{amb}(T - T_{amb}) + \epsilon \cdot \sigma \cdot \left(T^4 - T_{amb}^4\right) \tag{19}$$

at $r = r_{out}$, and

$$\frac{\partial T}{\partial r} = 0 \tag{20}$$

at $r = 0$.

The convective heat transfer coefficient to ambient (h_{amb}) is computed using the well-known relations for free and forced convection in external flows over cylinders [43].

The 2-dimensional temperature field in the cylindrical converter is solved using the alternative direction implicit (ADI) technique, which offers stability advantages without excessive computation effort.

3.2. Reaction scheme and kinetic rate expressions

As mentioned above, the kinetic rate expressions are probably the most crucial for the reliability of the computer model. Out of the multitude of the known reactions occurring on the catalytic surface, the following reaction scheme may be considered as fundamental, able to describe the basic chemistry of a typical automotive catalyst:

$$CO + 1/2O_2 \rightarrow CO_2 \tag{21}$$

$$H_2 + 1/2O_2 \rightarrow H_2O \tag{22}$$

$$C_xH_y + \left(x + \frac{y}{4}\right)O_2 \rightarrow xCO_2 + \frac{y}{2}H_2O \text{ — fast HC} \tag{23}$$

$$C_xH_y + \left(x + \frac{y}{4}\right)O_2 \rightarrow xCO_2 + \frac{y}{2}H_2O \text{ — slow HC} \tag{24}$$

$$C_xH_y + xH_2O \rightarrow xCO + \left(x + \frac{y}{2}\right)H_2 \text{ — fast HC} \tag{25}$$

$$2CO + 2NO \rightarrow 2CO_2 + N_2 \tag{26}$$

The definition of the reaction scheme was based on a compromise between minimization of the tunable parameters and model representability in real-world operating conditions. The 6-reaction scheme does not aim at describing the 3-way catalyst behavior under random operating conditions. However, 3-way catalysts operate at a relatively narrow range regarding exhaust gas composition, which is very close to stoichiometry. The exceptions are the transient fuel-cut phases during decelerations, as well as possible fuel enrichments during cold starts. We have further restricted our reaction scheme to the reactions, which are

significant for the main pollutants considered, e.g. CO, HC and NO_x. Hydrogen oxidation is taken into account, due to the substantial heat production associated with it, while its reaction kinetics are easy to handle, since they are closely related to CO oxidation kinetics [44]. The reaction with CO is considered as the main path for NO reduction, although other reducing species, such as hydrogen or hydrocarbons may also contribute to NO conversion. The high HC conversion efficiencies observed in fresh catalysts during operation in rich exhaust has been attributed to the steam reforming reaction [45,46], which has also been included in the reaction scheme.

The rate expressions used for the above reactions are the following:

$$R_1 = \frac{A_1 \cdot e^{-E_1/RT} \cdot c_{CO} \cdot c_{O_2}}{G_1} \tag{27}$$

$$R_2 = \frac{A_2 \cdot e^{-E_2/RT} \cdot c_{H_2} \cdot c_{O_2}}{G_1} \tag{28}$$

$$R_3 = \frac{A_3 \cdot e^{-E_3/RT} \cdot c_{C_xH_y} \cdot c_{O_2}}{G_1} \tag{29}$$

$$R_4 = \frac{A_4 \cdot e^{-E_4/RT} \cdot c_{C_xH_y} \cdot c_{O_2}}{G_1} \tag{30}$$

$$R_5 = \frac{A_5 \cdot e^{-E_5/RT} \cdot c_{C_xH_y} \cdot c_{H_2O}}{G_1} \mathrm{Eq}_5 \tag{31}$$

$$R_6 = A_6 \cdot e^{-E_6/RT} \cdot c_{CO}^{m} \cdot c_{NO}^{0.5} \tag{32}$$

with:

$$G_1 = T_s\left(1 + K_1 c_{CO} + K_2 c_{C_3H_6}\right)^2 \left(1 + K_3 c_{CO}^2 c_{C_3H_6}^2\right)\left(1 + K_4 c_{NO}^{0.7}\right) \tag{33}$$

The following expressions for the adsorption equilibrium constants are used for certain Pt containing catalysts [12,8]:

$$K_1 = 65.5 \exp(961/T)$$

$$K_2 = 2.08 \cdot 10^3 \exp(361/T)$$

$$K_3 = 3.98 \exp(11{,}611/T)$$

$$K_4 = 4.79 \cdot 10^5 \exp(-3733/T)$$

The form of the kinetic rate expression is the one proposed in [12], which has been extensively employed in previous models. In view of the lack of precise kinetic measurements concerning the steam reforming reaction [47], we use a rate expression containing the same inhibition factor as in the oxidation reactions. The rate expression for the steam reforming takes also the chemical

equilibrium of the reaction in account. This is accomplished by the factor Eq_5 appearing in (31) and is defined as [48]:

$$Eq_5 = 1 - \frac{c_{s,CO}^{x} \cdot c_{s,H_2}^{x+0.5y}}{c_{C_xH_y} \cdot c_{H_2O}^{x} \cdot K_p(T)} \tag{34}$$

Correlations for the chemical equilibrium constant $K_p(T)$ as function of temperature can be found in related handbooks [48]. Obviously, negative values for Eq_5 imply that the steam reforming reaction is thermodynamically not possible and the reaction rate is zero.

As regards the reaction rate expression for NO reduction by CO, the experimental findings given in [28] on Rh-based catalysts are exploited using a positive order for NO and a negative one for CO for the reaction conditions studied (CO concentration between 1 and 5 vol.-%, NO between 0.1 and 0.8 vol.-%). Since the operating conditions extend to lower concentration values in real world operation the results presented in [29] on Pt/Rh catalysts are exploited in this direction. According to these experimental results the reaction order for CO seems to approach unity when the reactant concentrations approach zero. This is mathematically expressed using the following relation for the exponent m in Eq. (32):

$$m = -0.19(1 - 6.26 \cdot e^{-m_1 \cdot c_{s,CO}}) \tag{35}$$

where m_1 is a tunable factor.

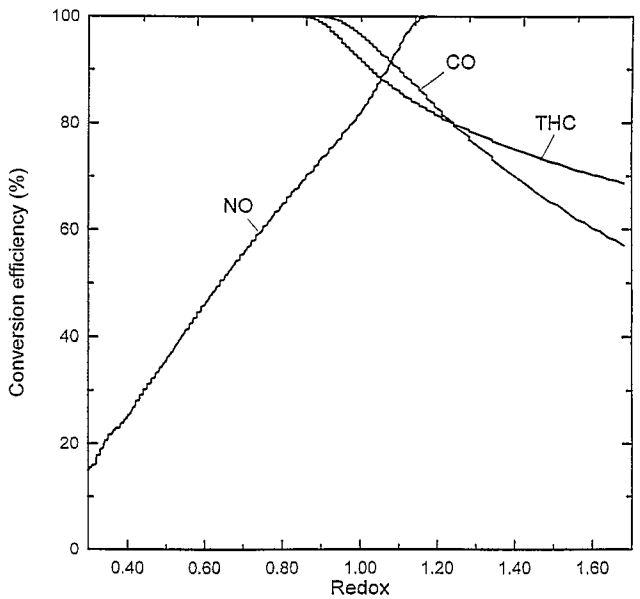

Fig. 1. Model predictions of converter efficiency under different exhaust gas inlet redox conditions. The exhaust gas inlet temperature is 500°C. Converter properties are given in Table 1.

A typical feature of the 3-way converter models is the ability to predict the 'lambda-window' behavior, i.e. the narrow air-to-fuel ratios around stoichiometry, where all the three main pollutants are converted with high efficiency. Fig. 1 presents the predicted CO, HC and NO conversion efficiency of a catalytic converter at 500°C for different exhaust gas redox conditions. The redox ratio is defined as:

$$\text{Redox} = \frac{c_{CO} + c_{H_2} + 6 \cdot \left(1 + \frac{\alpha}{4}\right) \cdot c_{HC}}{c_{NO} + 2 \cdot c_{O_2}} \tag{36}$$

Data regarding converter geometry and the constants used in the simulation

Table 1
Input data and constants regarding the catalytic converter used in the simulation tests presented

Input data		
Noble metal composition	Pt/Rh, 5:1	
Noble metal loading	50	g/ft^3
Monolith frontal area	0.01175	m^2
Monolith length	0.178	m
Channel density	400	channels/in^2
Substrate thickness	$0.154 \cdot 10^{-3}$	m
Washcoat layer thickness	$0.025 \cdot 10^{-3}$	m
Substrate density	1800	kg/m^3
Washcoat density	1000	kg/m^3
Monolith conductivity	1.5	W/m K
Monolith specific thermal capacity	1020	J/kg K
Insulation thickness	$3 \cdot 10^{-3}$	m
Insulation density	1000	kg/m^3
Insulation thermal conductivity	0.5	W/m K
Insulation specific thermal capacity	600	J/kg K
Heat convection coefficient to ambient	45	W/m^2 K
Emissivity of converter outer shell	0.3	
Oxygen storage capacity	10	mol/m^3

Kinetic constants		
Reaction	Activation energy E_i (J/mol)	Activity factor A_i (mol K/m^3 s)
1	95,000	$5 \cdot 10^{16}$
2	95,000	$5 \cdot 10^{16}$
3	105,000	10^{18}
4	125,000	$1.2 \cdot 10^{18}$
5	105,000	$1.7 \cdot 10^{12}$
6	70,000	$1.5 \cdot 10^{6}$

Constants in the oxygen storage submodel	
Activity factors (mol/m^3 s)	Activation energies (J/mol)
$A_{ox} = 9 \cdot 10^8$	$E_{ox} = 90{,}000$
$A_{red} = 3 \cdot 10^8$	$E_{red} = 90{,}000$

Table 2
Exhaust gas composition used for the simulation of the redox scan test

Gas	Percentage
CO	1.1
O_2	0.5–5
CO_2	14
H_2O	10
H_2	0.37
C_3H_8	0.016
C_3H_6	0.032
NO	0.1
N_2	balance

are given in Table 1. Table 2 contains the exhaust gas composition values used; the Redox is varied by variation of the oxygen concentration.

In order to give a more comprehensive explanation of the lambda window behavior, Fig. 2 presents the CO, O_2, NO profiles along the converter for redox values corresponding to lean, stoichiometric and rich conditions. At rich conditions (Redox > 1) the CO and HC conversion efficiency is limited by the availability of oxidizing species. At lean conditions (Redox < 1) CO is consumed by oxygen before NO is completely consumed. At a certain distance from the inlet, NO flows practically unreacted through the converter due to the absence of reducing species. The model accuracy in such tests relies on both representative kinetic expressions and on reliable simulation of the transport phenomena in the converter.

3.3. Oxygen storage submodel

The oxygen storage submodel used in the present work is rather phenomenological and aims at improving the model's prediction accuracy during critical transient operation modes. The independent parameters of the model are the minimum required and can be estimated for each case by standard measurements. Taking into account the analysis of the previous section, we consider that the oxygen storage mechanism may be described by the oxidation and reduction of the Ce oxides present in the washcoat according to the following reaction:

$$2CeO_2 \leftrightarrows Ce_2O_3 + \frac{1}{2}O_2 \tag{37}$$

The reaction to the right denotes the release of an oxygen atom, which is made available to react with a reducing species of the exhaust gas (e.g., CO). The left direction of the reaction represents the storage of an oxygen atom by increasing the oxidation state of Ce_2O_3. We define the auxiliary number ψ as:

$$\psi = \frac{2 \times \text{moles } CeO_2}{2 \times \text{moles } CeO_2 + \text{moles } Ce_2O_3} \tag{38}$$

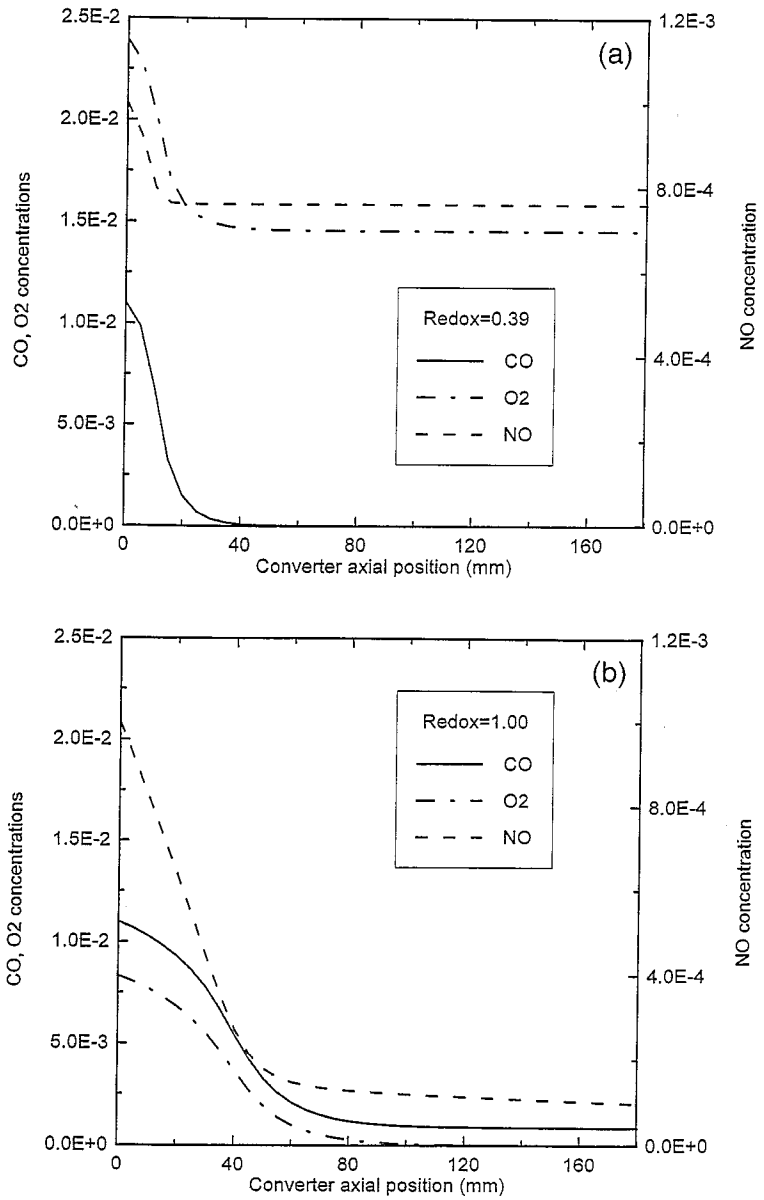

Fig. 2. Lambda-window behavior of the 3-way catalytic converter. CO, O_2 and NO profiles along the converter are computed for three different exhaust gas inlet redox values. (a) Redox = 0.39, (b) Redox = 1.00, (c) Redox = 1.73. Converter properties are given in Table 1.

which can be considered as the fractional extend of oxidation of the oxygen storage component. The extend of oxidation is changing continuously during transient converter operations and is affected by the relative reaction rates of Eq. (37).

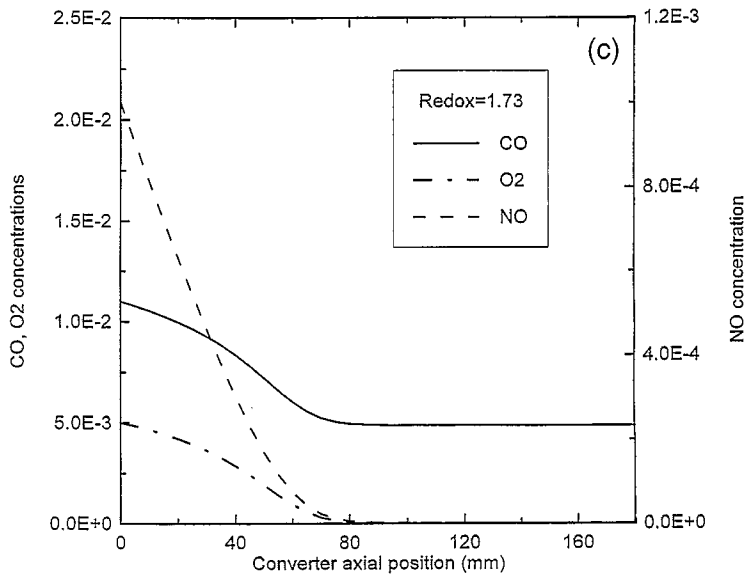

Fig. 2. (continued).

The oxidation rate is expected to be proportional to the available active sites of 'reduced-state' cerium oxides, which are expressed by the factor $\Psi_{cap}(1-\psi)$. The rate should be also dependent on the prevailing oxygen concentration at the gas–solid interface. The linear dependence on O_2 concentration is considered as a realistic assumption. The oxidation reaction rate is thus:

$$R_{ox} = k_{ox}(T)c_{s,O_2}\Psi_{cap}(1-\psi) \tag{39}$$

where k_{ox} is a characteristic rate constant, which exhibits an Arrhenius type dependence on temperature:

$$k_{ox} = A_{ox} \cdot e^{-E_{ox}/RT} \tag{40}$$

Analogous considerations are made for the reduction reaction rate. Here, the rate is expected to be directly proportional to $\Psi_{cap}\psi$, and should exhibit a dependence on the local CO concentration:

$$R_{red} = k_{red}(T)c_{CO}\Psi_{cap}\psi \tag{41}$$

with

$$k_{red} = A_{red} \cdot e^{-E_{red}/RT} \tag{42}$$

The variation of the oxidation extend Ψ should be computed at each location by the following differential equation:

$$\frac{d\psi}{dt} = -\frac{R_{red}}{\Psi_{cap}} + \frac{R_{ox}}{\Psi_{cap}} \tag{43}$$

which is solved numerically by the implicit Euler method for each node.

Fig. 3 presents the amount of oxygen stored in the catalyst during a gradual temperature increase of the inlet gas temperature. Three tests with different exhaust gas redox values are simulated. The dependence of the oxygen availability on temperature and redox predicted by the model are in accordance with previously published observations [39]. Under lean conditions (Redox = 0.63) the amount of the stored oxygen is determined by the Arrhenius-type temperature dependence of Ce oxidation kinetics. The abundance of oxygen in the feed gas produces much higher Ce oxides oxidation than the reduction rates. This results in complete Ce oxidation for high enough temperatures. For exactly stoichiometric conditions, oxygen storage competes with the oxidation reactions for the consumption of oxygen. The result is that only a fraction of the total oxygen storage capacity is available during stoichiometric operation, even in the high temperature region. Under rich operation modes the oxygen storage availability initially increases with temperature, according to the Ce oxidation kinetics. Due to the high competition, the Ce oxidation rates are lower, but still observable until a temperature of about 300°C. After this temperature level, the oxidation of slower hydrocarbons becomes significant so that there is no oxygen left to be stored. In the high temperature region there is virtually no oxygen stored on the washcoat.

Following the above discussion, it can be summarized that the model is able to simulate, at least qualitatively, the main transient phenomena attributed to oxygen storage effects. In order to represent the actual behavior of different

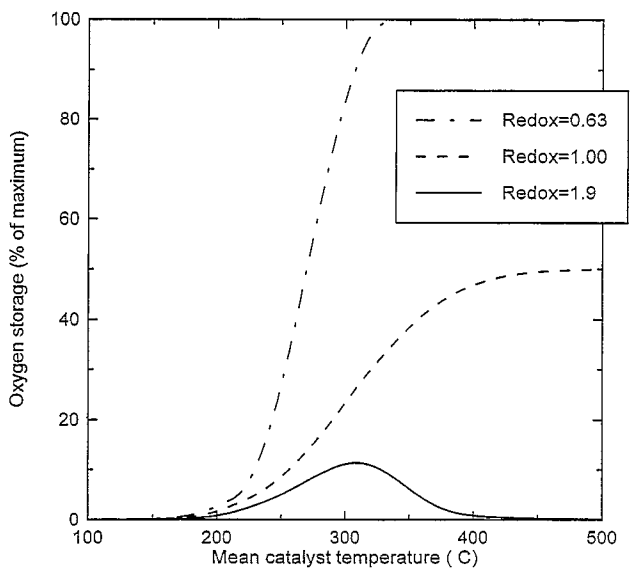

Fig. 3. Computed availability of stored oxygen as function of catalyst temperature and exhaust gas redox. Converter properties are given in Table 1.

catalyst formulations, the oxygen storage model kinetic parameters should be determined. This is a task involving interaction between experiments and calculation, which is a subject of another research work [49].

4. Model application range

In this section, selected application examples are presented to illustrate the scope and extends of the model exploitation. Although the applications presented below refer to gasoline fueled engines fitted with conventional catalytic converters, the modeling approach presented is flexible in simulating a variety of catalyst formulations with alternative fuel engine exhaust (CNG, methanol etc.).

4.1. Emission prediction over driving cycles

The chemical engineer involved in pollution control is highly interested in the prediction of converter efficiency over full driving cycles, by employing both computation and limited testing. The results of a common application of the converter model and computer code is shown in Fig. 4. In this figure the CO, HC and NO cumulative emissions downstream the catalyst are plotted vs. time

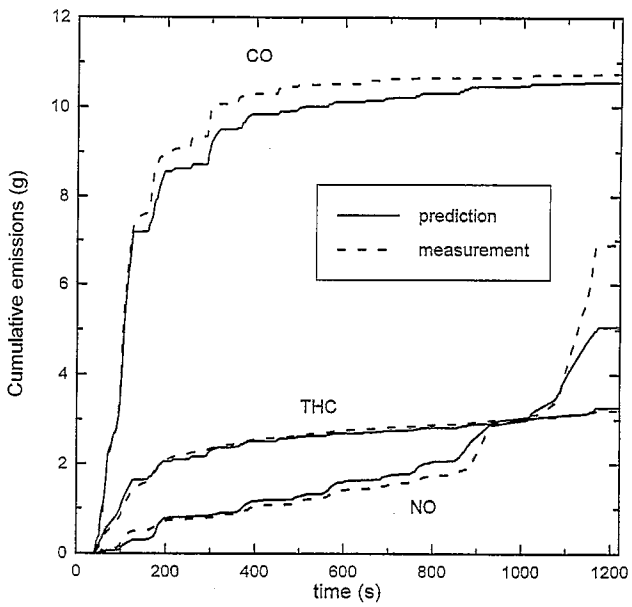

Fig. 4. Cumulative CO, HC, NO emissions in the new european legislated driving cycle (NEDC) for a 2-l engined gasoline car. Model predictions vs. measurements.

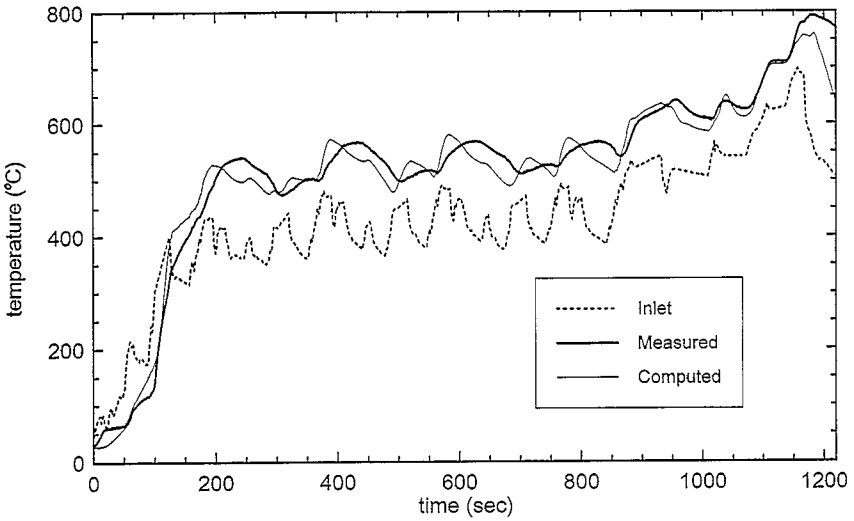

Fig. 5. Comparison of measured vs. model predicted exhaust gas temperatures at 50 mm from the catalyst inlet face. The exhaust gas temperature at the converter inlet is also plotted on the graph. The test is the same as the one referred to in Fig. 4.

during a full legislated european driving cycle (NEDC). Additionally, Fig. 5 presents a comparison between the measured and computed gas temperatures 50 mm from the catalyst inlet. The following remarks should be made regarding the model application in such cases:

(i) a large amount of input data (time resolved values of the inlet temperature, flow rate and composition of the exhaust gas) is required for such applications. Modal analysis providing exhaust gas composition averaged over distinct driving operation modes (idling, acceleration, constant speed, deceleration) does not usually suffice for modeling purposes. Since a significant portion of the total tailpipe emissions in such systems arise from highly transient short duration modes (braking with fuel cut-off, abrupt load changes with poor stoichiometry control), it is critical to have time resolved input data at a minimum of 1 Hz acquisition;

(ii) the hydrocarbon composition in the exhaust gas is a function of the engine temperature and operation point. With conventional analyzers it is not possible to have time-dependent information about the different activity hydrocarbons present in the exhaust. Usually, the hydrocarbons are classified a priori in two categories (fast and slow reacting) based on the experience of the engine out emissions under consideration. This is, however, one of the rougher approximations made in such computations. The respective model sensitivity is illustrated in Fig. 6, which compares the predicted cumulative emissions in an NEDC for different approximations in the fast to slow hydrocarbons fraction used. The resulting accuracy limitations may be overcome by the knowledge of time-dependent hydrocarbon composition at the catalyst inlet;

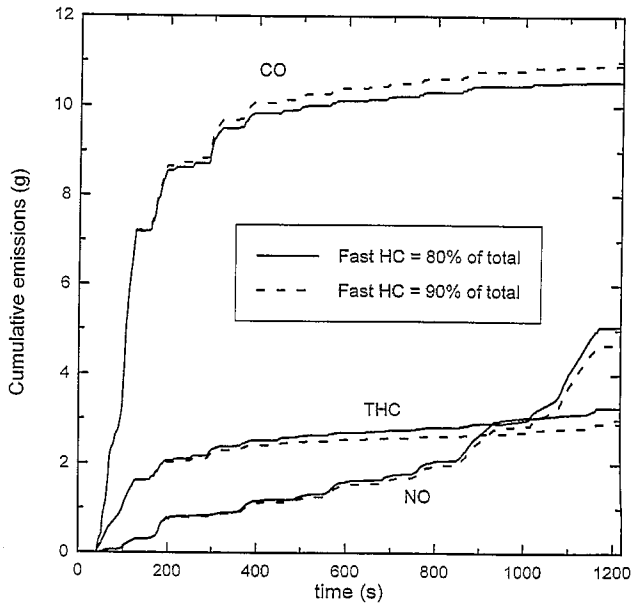

Fig. 6. Model sensitivity on the fraction of fast/slow hydrocarbons. Comparison of predicted cumulative HC emissions of a 2-l engined gasoline car emissions in the new european legislated driving cycle (NEDC).

(iii) in order to assess the overall CO and HC converter efficiency, the model should be accurate in predicting both the appearance of catalyst light-off as well as the catalyst performance during engine transients accompanied with instantaneous oxygen shortage in the exhaust. The prediction of catalyst light-off requires accurate kinetic constants for the oxidation reactions, which may be derived with the help of laboratory catalytic activity measurements [49]. On the other hand, the critical model for highly transient operations is the oxygen storage submodel. Fig. 7 illustrates the importance of correctly assessing the oxygen storage parameters. Especially, the CO emissions are highly sensitive to the oxygen storage effects. Abrupt changes in operating mode are accompanied by deviations of the exhaust gas mixture from stoichiometry, due to the inability of the fuel injection system to respond accurately to such fast changes. The steam-reforming reaction contributes to hydrocarbon conversion even under oxygen shortage conditions. On the other hand, CO can be consumed during short duration rich excursions mainly via the oxygen storage mechanisms, thus being more sensitive to the oxygen storage capacity of the catalyst;

(iv) NO emissions are less affected by the catalyst light-off, since NO engine out emissions are very low for engine operation at low loads, which is the case during the first seconds after the cold start in a legislated cycle. During high load engine operation, when NO engine out emissions become significant, their conversion efficiency is practically limited by the availability of reducing agents, mainly CO. Consequently, the prediction of NO conversion prerequisites

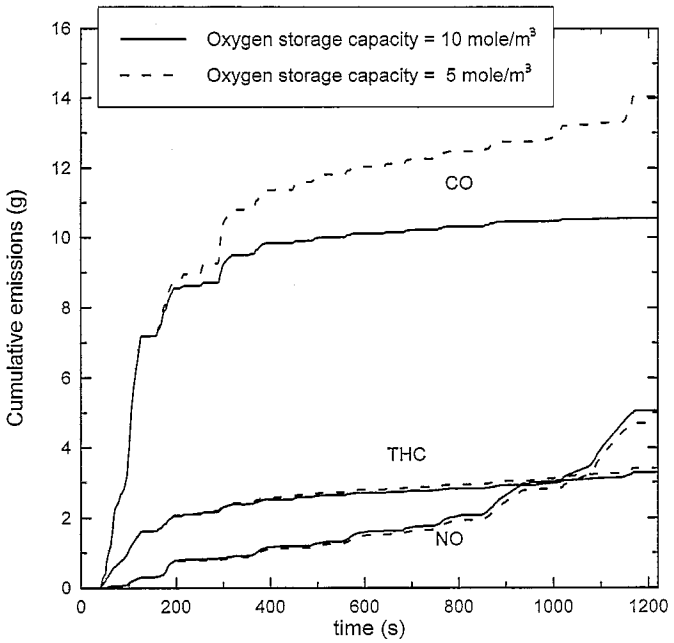

Fig. 7. Computed effect of oxygen storage capacity of the converter on the cumulative emissions of the 2-l engined gasoline car emissions in the new european legislated driving cycle (NEDC).

accurate kinetic expressions for both CO consumption and NO reduction reactions.

4.2. Comparative assessment of fast light-off techniques

The attainment of stricter emission standards for gasoline vehicles is based on the reduction of cold start emissions by the achievement of faster light-off. Several passive and active systems have been presented during the last years in the literature. The optimum selection of the design and operating parameters involved in these 'fast light-off techniques' can be substantially aided by computational investigations [50].

A common technique for achieving faster light-off is the installation of an additional, thermally stable, close coupled pre-catalyst of smaller volume. Model runs can be employed to assess the effect of several geometrical parameters of the pre-catalyst, e.g., volume, substrate cell density and wall thickness. Fig. 8 presents, as an illustrative example, the computed cold start HC emissions as a function of the pre-converter volume, for two substrate geometries. The HC emissions present an asymptotic behavior regarding the pre-converter volume, which agrees with the trend to employ small volume catalysts in these cases [51,52]. The beneficial effects of using lower mass and higher cell density

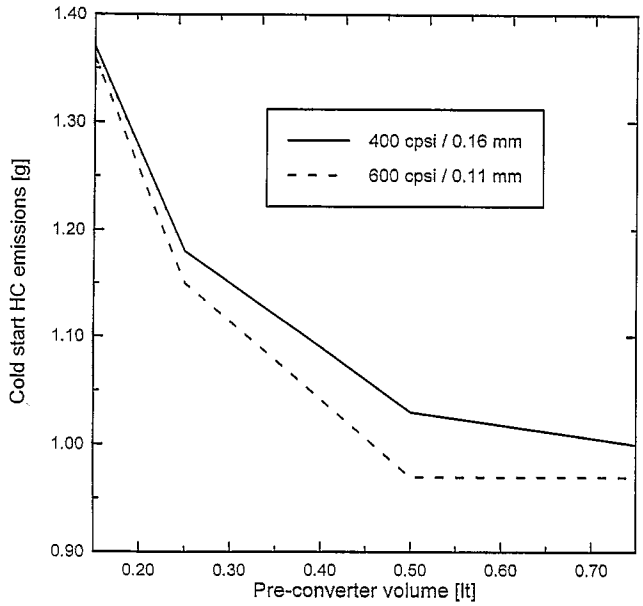

Fig. 8. Model application in the design of pre-converter fast light-off systems. Effect of pre-converter volume and substrate geometry (channel density, wall thickness) on cold start HC emissions. The remaining pre-converter properties are the same as that of the main converter (Table 1).

substrates can be quantitatively assessed, regarding catalyst performance during standard driving cycles.

Obviously, there are still some parameters affecting the design of pre-catalysts, that should be additionally taken into account in such cases. These parameters, regarding backpressure effects on engine performance, mechanical and thermal stability and cost, require separate optimization work.

The purpose of these computations is to reveal critical trends, which may help in avoiding a great deal of experimental effort and shorten the system development time. A multitude of similar optimization applications may be supported by the model, e.g., determination of optimum heating scenarios in electrically heated catalysts, comparative assessment of different substrates.

4.3. Effects of flow pattern at the converter inlet

Previous investigations have addressed the effect of exhaust gas flow maldistribution at the catalyst face on the efficiency under steady-state operating conditions [11,24,53]. The 2-dimensional model is able to account for the effects of non-uniform flow distribution as well as for heat losses to the environment and the resulting radial temperature gradients in the monolith.

The higher temperatures in the region of the converter axis favor increased conversion efficiency. On the other hand, the outer channels are generally subjected to lower local flow rates, thus operating with lower space velocities,

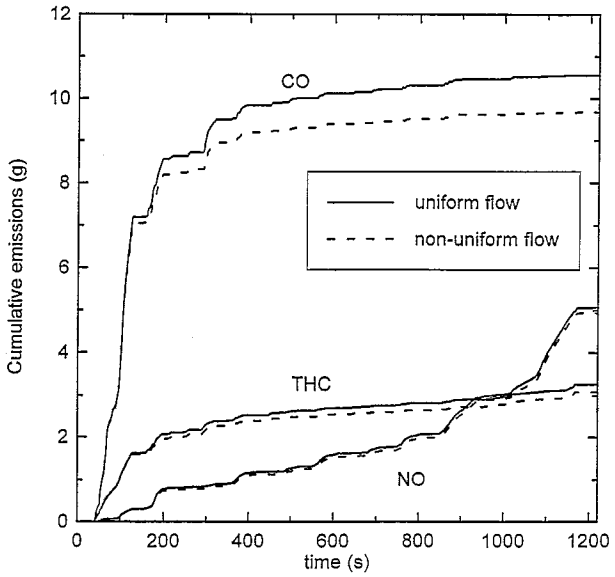

Fig. 9. Comparison of model predictions for uniform and non-uniform flow distribution at catalyst inlet face. It may be observed, that under the examined operating conditions, the specific flow maldistribution profile shows a slightly improved performance.

which partially make up for the effect of lower temperature levels. Apart from recognizing and quantifying the effects of flow distribution in steady-state operation, the 2-D transient model may assess the importance of optimizing the flow pattern at the catalyst inlet, as regards the overall emissions in legislated driving cycles.

Fig. 9 compares model predictions over an NEDC for different flow patterns at the monolith face. For the simulation of the non-uniform flow distribution the axial velocity profile along the monolith diameter is considered parabolic and the velocity values taken at the monolith center and outer radii are 1.4 and 0.6 times the mean axial velocity respectively. It can be recognized that the concentration of the major exhaust gas flow portion in the inner, warmer monolith channels presents observable advantages as regards the CO light-off. Hydrocarbon emissions exhibit similar behavior, whereas NO emissions, which are less sensitive to temperature levels are practically unaffected by the flow maldistribution. The locally high space velocities in the inner channels are not enough to result to a catalyst breakthrough during the hot mode of the cycle; the catalyst volume of the 2-l car is sufficient to prevent any breakthroughs at the relatively low flow rates observed in this cycle.

4.4. Prediction of catalyst thermal loading — catalyst ageing

The operation of the converter under the severe exhaust gas composition, temperature and flow rate transients resulting from engine misfiring is a subject

of importance in the investigation of converter durability [54]. Similarly, high catalyst temperatures may be developed during fuel cut-off operating modes associated with vehicle deceleration. Since these effects may prove detrimental for a useful catalyst life, the study can be substantially aided by the use of advanced models for transient 3-WCC operation [55].

The model may be further employed in the assessment and design of accelerated converter ageing procedures, which are routinely employed by the catalyst and automotive manufacturers, in order to assess catalyst durability avoiding the time and cost intensive mileage accumulation tests [56]. An accelerated ageing cycle should be suitably designed in order to subject the catalyst to temperature levels equivalent to those expected during operation on the vehicle for a useful converter life. The catalyst thermal loading is a complex function of its chemical activity as well as of the feed gas inlet conditions; moreover, the converter is aged non-uniformly both axially and radially. The converter model could be conveniently employed for the prediction of the catalyst thermal loading and thus avoid many time consuming procedures in the process of converter durability assessment and optimum selection. More details about the procedures employed and the role of model predictions in such applications are given elsewhere [57].

5. Discussion

Mathematical models of the transport and chemical phenomena in automotive catalysts have been successfully employed in the past for converter operation under oxygen abundance conditions. The case of 3-way catalysts operating under both oxidizing and reducing atmosphere is obviously more complicated. Further difficulties arise from the uncertainties in chemical kinetics for the multitude of catalyst formulations and ageing modes. The published work regarding reaction kinetics and modeling in 3-way catalysts has been relatively limited.

The model presented in this work relies on dimensionless Nu and Sh number correlations to calculate the heat and mass transfer in the converter channels, instead of solving the laminar boundary layer profiles of temperature and concentration. This is currently a commonly-accepted approach and is considered sufficient for the desired accuracy levels. The converter heat losses effects are generally quite important and should be suitably handled with the solution of the 2-dimensional temperature field in the converter. The 2-dimensional approach is useful in estimating the effect of flow distribution at the converter inlet. However, a prediction or measurement of velocity profiles at the inlet under a variety of operating modes and exhaust line geometries is necessary as input in this case.

Kinetic expressions are probably the most crucial data for model reliability.

These data are certainly different from one catalyst to the other. However, the reactions are the same and the catalyst formulations may be clustered in a few main categories. This suggests that the structures of the rate expressions are probably independent of the catalyst, whereas the parameters involved are dependent. This approach seems to be more realistic at the present stage for catalyst modeling purposes. Well designed laboratory tests may be used in co-operation with mathematical models to yield approximations of the main reaction kinetics parameters [49].

The definition of the reaction scheme was based on a compromise between minimization of the tunable parameters and model representability in real-world operating conditions. The 6-reaction scheme describes with sufficient accuracy the 3-way catalyst behavior under the operating conditions usually found in gasoline car applications. A new feature in comparison with previous modeling studies is the inclusion of the steam-reforming reaction. This allows a better prediction of the high HC conversion efficiencies observed in fresh catalysts during operation in rich exhaust.

Converter operation under transient exhaust composition is significantly affected by the oxygen storage characteristics. A comprehensive model considering a simplified mechanism of Ce oxidation and reduction is employed in the present work. Comparisons with experimental results are rather encouraging in this respect. Other transient phenomena (noble metal periodic oxidation–reduction) may also be important for the prediction of converter efficiency under cycling exhaust gas conditions. These require, however, further experimental evidence in order to include in the mathematical model.

The reaction with CO is considered as the main path for NO reduction, although other reducing species, such as hydrogen or hydrocarbons may also contribute to NO conversion. The kinetic expressions for NO reduction presents greater difficulties due to the high redox sensitivity and the complex dependence on CO availability. The experimental work of previous researchers has been exploited to develop a rate expression covering both oxidizing and reducing conditions.

The main purpose of this paper was the investigation of model applicability to the range of possible engineering applications. The requirements in accuracy of the input data vary according to the application examined. Although the task of predicting emissions over random driving scenarios is quite demanding in both chemical kinetics and inlet conditions data, most optimisation applications may be sufficiently handled with existing kinetic expressions information.

Possible directions of future work on the subject may be focused on the investigation of transient catalyst features during cycling exhaust conditions in order to explain relevant phenomena and possibly optimise engine fuelling strategies. The assessment of the critical kinetic rate parameters by combining model and experimental results could be based on specially designed laboratory tests. The latter is a subject of the authors' work in the near future.

6. Nomenclature

6.1. Variables

3-WCC	3 way catalytic converter
A	reaction rate constant, mol K/m^3 s
$\bar{c}_s$	vector including species concentrations, mole fraction
c	species concentration, mole fraction
C_p	specific heat capacity, J/kg K
ΔF	elementary exchange area, m^2
ΔH	reaction enthalpy, J/mol
ΔV_r	elementary reactor volume, m^3
d	diameter, m
D	mass diffusivity, m^2/s
Eq	reaction rate factor accounting for chemical equilibrium
F	exchange area, m^2
G	inhibition factor, K
Gz	Graetz number
h	convective heat transfer coefficient, W/m^2 K
k	mass transfer coefficient, m/s
k_{ox}	oxygen storage component oxidation rate constant, mol/m^3 s
k_{red}	oxygen storage component reduction rate constant, mol/m^3 s
K	adsorption equilibrium constant
K_p	chemical equilibrium constant
l	length, m
$\dot{m}$	mass flow rate, kg/s
M	molecular weight, kg/mol
$\dot{n}$	molecular flux, mol/m^3 s
NEDC	New European Driving Cycle
NTU	number of transfer units
Nu	Nusselt number, Nu $= (h \cdot d_h)/(\lambda_g)$
Pe	Peclet number, Pe = Re Pr
$\dot{q}$	heat transfer rate, W/m^3
r	radius, m
R	reaction rate or gas constant, mol/m^3 s or J/mol K
S	heat source term, W/m^3
Sh	Sherwood number, Sh $= (k \cdot d_h)/(D)$
t	time, s
T	temperature, K
W	parameter used in the mass balance equation, $(\dot{m}_g)/(\Delta V_r M_g)$ $(1 - e^{-NTU_m})$
x	carbon atoms in the hydrocarbon molecule, axial distance, m

x^* dimensionless axial distance, $x^* = (x)/(d_h \cdot \mathrm{Pe})$
y hydrogen atoms in the hydrocarbon molecule

6.2. Greek letters

α average hydrogen-to-carbon ratio of the exhaust gas hydrocarbons
ϵ emissivity factor (radiation)
λ thermal conductivity, W/m K
ρ density, kg/m^3
σ Stefan–Boltzmann constant, $W/m^2\ T^4$
ψ oxidation fraction

6.3. Subscripts

amb ambient
cap capacity
conv convection
el electric
g exhaust gas
h hydraulic or heat
i space node index
j indication of exhaust species
k indication of reaction k (Eqs. (21)–(26))
m mass
out outer
ox oxidation
red reduction
s solid

Acknowledgements

Part of the work described in this paper was carried out in the frame of two Brite-EuRam II European Community funded projects (BE-5547, BE-7142). The authors wish to thank EU-DG XII for their financial assistance in these projects.

References

[1] L.C. Young and B.A. Finlayson, AIChE J., 22(2) (1976) 331–343.
[2] R.H. Heck, J. Wei and J.R. Katzer, AIChE J., 22(3) (1976) 477–484.

[3] S.T. Lee and R. Aris, Chem. Eng. Sci., 32 (1977) 827–837.
[4] N.O. Otto and W.J. LeGray, SAE paper 800841 (1980).
[5] S.H. Oh, J.C. Cavendish and L.L. Hegedus, AIChE J., 26 (1980) 935.
[6] S.H. Oh and J.C. Cavendish, AIChE J., 31(6) (1985) 935–942.
[7] S.H. Oh and J.C. Cavendish, AIChE J., 31(6) (1985) 943–947.
[8] S.H. Oh and J.C. Cavendish, Ind. Eng. Chem. Prod. Res. Dev., 21 (1982) 29–37.
[9] M. Flytzani-Stephanopoulos, G.E. Voecks and T. Charng, Chem. Eng. Sci., 41 (1986) 1203–1212.
[10] E.R. Becker and K. Zygourakis, Monolith Catalyst Design Options for Rapid Light-Off, presented at the 1986 Annual Meeting of AIChE, Miami Beach, FL, 1986.
[11] D.K.S. Chen, E.J. Bissett, S.H. Oh and D.L. Van Ostrom, SAE paper 880282 (1988).
[12] S.E. Voltz, C.R. Morgan, D. Liederman and S.M. Jacob, Ind. Eng. Chem. Prod. Res. Dev., 12 (1973) 294.
[13] D.K.S. Chen and C.E. Cole, SAE paper 890798 (1989).
[14] I. Gottberg, J.E. Rydquist, O. Backlund, S. Wallman, W. Maus, R. Brueck and H. Swars, SAE paper 910840 (1991).
[15] C. Montreuil, S. Williams and A. Adamszyk, SAE paper 920096 (1992).
[16] K.N. Pattas, A.M. Stamatelos, P.K. Pistikopoulos, G.C. Koltsakis, P.A. Konstantinidis, E. Volpi and E. Leveroni, SAE paper 940934 (1994).
[17] S. Siemund, D.J. Schweich, P. Leclerc and J. Villermaux, Stud. Surf. Sci. Catal., 96 (1995) 887.
[18] D. Schweich, Stud. Surf. Sci. Catal., 96 (1995) 55.
[19] R.D. Hawthorn, AIChE Symp. Ser., 70 (1974) 428–438.
[20] J.R. Mondt, Trans. ASME: J. Eng. Gas Turbines Power, 109 (1987) 200–206.
[21] L.C. Young and B.A. Finlayson, Appl. Automobile Exhaust AIChE J., 22(2) (1976) 343–353.
[22] R.E. Hayes and S.T. Kolaczkowski, Chem. Eng. Sci., 49(21) (1994) 3587–3599.
[23] G. Groppi, A. Belloli, E. Tronconi and P. Forzatti, Chem. Eng. Sci., 50(17) (1995) 2705–2715.
[24] G. Bella, V. Rocco and M. Maggiore, Trans. ASME: J. Eng. Gas Turbines Power, 113 (1991) 419–426.
[25] M.C. Lai, T. Lee, J.Y. Kim, C.Y. Cheng, P. Li and G. Chui, J. Fluids Struct., 6 (1992) 451–470.
[26] H. Weltens, H. Bressler, F. Terres, H. Neumeier and D. Rammoser, SAE paper 930780 (1993).
[27] B. Subramanian and A. Varma, Ind. Eng. Chem. Prod. Res. Dev., 24 (1985) 512–516.
[28] S.H. Oh, J. Catal., 124 (1990) 477–487.
[29] E. Koberstein and G. Wannemacher, Stud. Surf. Sci. Catal., 30 (1987) 155.
[30] J.W. Bozek, R. Evans, C.D. Tyree and K.I. Zerafa, SAE paper 920289 (1992).
[31] R.K. Herz, J.B. Klela and J.A. Sell, Ind. Eng. Chem. Prod. Res. Dev., 22 (1983) 387–396.
[32] K.C. Taylor and R.M. Sinkevitch, Ind. Eng. Chem. Prod. Res. Dev., 22 (1983) 45–51.
[33] J.C. Schlatter, R.M. Sinkevitch and P.J. Mitchell, Ind. Eng. Chem. Prod. Res. Dev., 22 (1983) 51–56.
[34] Matsunaga Schin-ichi, K. Yokota, H. Muraki and Y. Fujitani, SAE paper 872098 (1987).
[35] H. Katashiba, M. Nishida, S. Washino, A. Takahashi, T. Hashimoto and M. Miyake, SAE paper 910390 (1991).
[36] A.F. Diwell, R.R. Rajaram, H.A. Shaw and T.J. Truex, Stud. Surf. Sci. Catal., 71 (1991).
[37] J.G. Nunan, H.J. Robota, M.J. Cohn and S.A. Bradley, Stud. Surf. Sci. Catal., 71 (1991).
[38] R.K. Herz, Ind. Eng. Chem. Prod. Res. Dev., 20 (1981) 451–457.
[39] G. Smedler, S. Eriksson, M. Lindblad, H. Bernler, S. Lundgren and E. Jobson, SAE paper 930944 (1993).
[40] S.H. Oh, G.B. Fisher, J.E. Carpenter and D.W. Goodman, J. Catal., 100 (1986) 360–376.
[41] A.B.K. Lie, J. Hoebink and G.B. Marin, Chem. Eng. J., 53 (1993) 47–54.
[42] R.K. Herz, Stud. Surf. Sci. Catal., 30 (1987) 427.
[43] W.M. Kays and M.E. Crawford, Convective Heat and Mass Transfer, 3rd ed., McGraw-Hill, 1993.
[44] D.W. Dabill, S.J. Gentry, H.B. Holland and A. Jones, J. Catal., 53 (1978) 164.
[45] J.C. Summers and R.G. Silver, SAE Trans., 99 (4) (1990) 556–567, SAE paper 902072.
[46] J. Barbier, Jr. and D. Duprez, Appl. Catal. B, 3 (1993) 61–83.
[47] J. Barbier, Jr. and D. Duprez, Appl. Catal. B, 4 (1994) 105–140.
[48] M.V. Twigg, Catalyst Handbook, 2nd ed., Wolfe, 1989.
[49] G.C. Koltsakis, P.A. Konstantinidis and A.M. Stamatelos, Chem. Eng. Commun., (1996) submitted.
[50] P.A. Konstantinidis, G.C. Koltsakis and A.M. Stamatelos, Proc. IMechE: J. Automobile Eng., in print.
[51] J.C. Summers, J.F. Skowron and M.J. Miller, SAE paper 930386 (1983).
[52] R.J. Locker, P.M. Then and U. Zink, SAE paper 960262 (1996).

[53] K. Zygourakis, Chem. Eng. Sci., 44(9) (1989) 2075–2086.
[54] S.H. Oh, SAE paper 881591 (1988).
[55] U. Spicher and G. Lepperhoff, Motortechn. Z., 56 (1995) 6.
[56] J. Siebler, M. Schreiner, R. Zimmer, M. Rieser, A. Hirschmann, G. Loose and H. Richter, Motortechn. Z., 55 (1994) 4.
[57] K.N. Pattas, A.M. Stamatelos, G.C. Koltsakis, P.A. Konstantinidis, E. Volpi and E. Leveroni, SAE paper 950934 (1995).